PRODUCTION OF η AND η' MESONS IN $\bar{p}p$ ANNIHILATION AT REST*

E. KLEMPT

Institut für Physik, Johannes-Gutenberg-Universität
55099 Mainz, Germany

(Received July 22, 1993)

The determination of the pseudoscalar mixing angle from η and η' production in proton–proton collisions and the extraction of the $\pi\pi$ and $\pi\eta$ phase shifts at low energies are central topics of the experimental program at COSY. These mesons are produced abundantly in $\bar{p}p$ annihilation at rest. The kinematical differences of the two production modes are pointed out. The extraction of the pseudoscalar mixing angle from branching ratios for $\bar{p}p$ annihilation requires dynamical corrections due to the fact that the η and η' have different masses. It is argued that the test of dynamical corrections is important for our understanding of NN and $N\bar{N}$ interactions.

PACS numbers: 13.75. Lb, 25.80. Hp

1. Light meson production in $p\bar{p}$ and pp interactions

NN and $N\bar{N}$ interactions are related by the G-parity rule, and the production of η and η' mesons in proton–proton interactions or in $\bar{p}p$ annihilation are conceptually similar processes. However, the differences between the two processes are striking: The available phase space in $\bar{p}p$ annihilation at rest is much larger than in pp interactions at COSY energies: the largest meson mass which can be produced at COSY is slightly above 1 GeV/c^2, at LEAR it is 2.4 GeV/c^2 (1.7 GeV/c^2 for annihilation at rest). This results in a larger variety of final states in $\bar{p}p$ annihilation, but also in a higher complexity of the data. Further, in $\bar{p}p$ annihilation there are no baryons in the final state, and hence there are no baryon resonances produced which might complicate the interpretation of η and η' production rates in proton–proton induced reactions.

* Presented at the Meson–Nucleus Interactions Conference, Cracow, Poland, May 14–19, 1993.

In any case, η and η' mesons are produced abundantly in $\bar{p}p$ annihilation. So the question arises if the the pseudoscalar mixing angle can be determined from this data. One should expect a strong energy dependence of meson production rates. This energy dependence is not known, so it has to be extracted from the data. Since the experimental groups at COSY will face similar problems I will discuss this aspect in some detail.

Since I suppose that most physicists in the audience are not familiar with the physics of $\bar{p}p$ annihilation I will shortly summarize the processes which precede the moment in which low-mass mesons are created [1].

2. Life history of an antiproton stopping in LH_2

Antiprotons are produced at CERN by bombarding a Cu target with protons accelerated to 26 GeV/c in the Proton Synchrotron. The antiproton momentum distribution shows a flat peak at 2.6 GeV/c. The breakthrough of antiproton physics is due to the development of the technique of phase space cooling [2] (for which S. van der Meer received the 1985 Nobel prize). This technique allows to collect antiprotons in a wide-acceptance Antiproton Collector, to transfer them to an Antiproton Accumulator, and to shrink the beam to monoenergetic pencil beams.

After accumulation the antiproton beam is transferred back to the PS where can be decelerated to 600 MeV/c and then passed to the Low–Energy–Antiproton–Ring (LEAR). The antiproton beam is then further cooled and — in case of the experiments described here — decelerated to 200 MeV/c. Then slow extraction starts (the extraction time last about one hour!) providing intense (up to 10^7 $\bar{p}$'s /s) and monoenergetic ($\delta p/p \leq 10^{-3}$) antiproton beams. The whole complex of PS, AC, AA and LEAR hence acts as a Tandem accelerator, but for *antiprotons* instead of protons.

Low-energy antiprotons entering a LH_2 target loose energy by ionization; they are moderated to energies of a few eV and then captured in the Coulomb field of a H atom by Auger effect (by ejection or excitation of an electron or chemical dissociation of a H_2 molecule) thus forming highly excited antiprotonic hydrogen ($\bar{p}p$) atoms. In LH_2 $\bar{p}p$ atoms undergo frequent collisions in which they experience intense electric fields. Thus Stark mixing between atomic levels of different orbital angular momenta occurs, and the $\bar{p}p$ atom has the chance to populate, in very high Rydberg states, a state with no orbital angular momentum (S state). From S states, annihilation occurs nearly instantly; and even from high-n P states there is a considerable chance for annihilation. The frequencies of S and P wave capture is not precisely known; the best guess is at present that $\sim$ 90% of all annihilation occur from S wave, 10% from P wave orbitals [3].

The $\bar{p}p$ annihilation process is not yet understood. Even worse, there is even no accepted picture of annihilation dynamics. The large number

of final states may suggest use of statistical models [4]; on the other hand, annihilation seems to be dominated by two-body intermediate states [5]. Possibly, the process can be described in the conventional picture of mesons and baryons [6], but many authors attempt a description in terms of quarks and gluons [7]. Dynamical selection rules are used to argue that SU(3) symmetry is important in p̄p annihilation [8]. In quark models there are rearrangement diagrams or annihilation diagrams [9]; their fractional contributions are discussed controversially. In two-meson annihilation, at least one $q\bar{q}$ pair annihilates; the annihilation vertex can either be described by an effective one-gluon operator [10], or one may assume that the $q\bar{q}$ pair annihilates into many gluons carrying vacuum quantum numbers [11]. A full model of p̄p annihilation needs in addition to take into account the possibility of initial state [12, 13]and final state [14] interactions. So annihilation seems to be sufficiently complex to exclude extraction of any useful information.

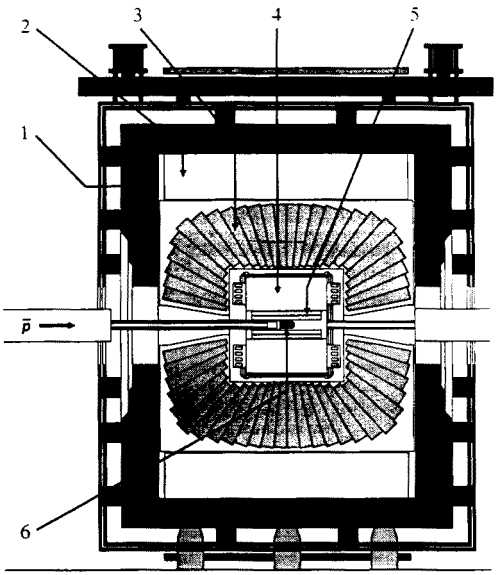

Fig. 1. Side view of the Crystal Barrel Detector with 1 Magnet yoke, 2 Magnet aluminium coil, 3 CsI electromagnetic calorimeter, 4 Jet Drift Chamber, 5 Proportional Wire Chambers, and 6 LH_2 target.

Phenomenologically, annihilation is observed into a multitude of different final states, see Fig. 1. The mesons shown in this Figure are stable against hadronic decays; but not against decays through electromagnetic or weak processes. In particular the π^0's will decay practically instantaneously into photons while the life time of charged pions and kaons allows

direct detection. Hence the observable relics of the annihilation process are charged pions and kaons and photons. Of particular interest for the present discussion are events in which no charged particles are produced. These comprise about 3.5% of all annihilation. By triggering on events with no charged particles in the final state, this annihilation mode can be analysed with high statistical power.

3. The Crystal Barrel experiment at LEAR

The extracted antiproton beam passes a beam line, a trigger scintillator and then enters a liquid H_2 (LH_2) target situated in the center of the Crystal Barrel detector (see Fig. 1). The target is surrounded by two Multi-Wire Proportional Chambers (MWPC) and a Jet Drift Chamber (JDC). The distinctive component of the Crystal Barrel detector is a calorimeter consisting of 1380 CsI crystals which all point at the H_2 target in the center of the detector. The assembly of H_2 target, MWPC's, JDC and CsI crystals is surrounded by a solenoidal magnet providing a field of 1.5 Tesla. A full description of the detector can be found elsewhere [15].

4. Production of η and η' mesons

The data presented below were recorded with the Crystal Barrel detector and a trigger on annihilations into photons only. About 7 000 000 events were written to tape. This corresponds to 220 000 000 $\bar{p}p$ annihilations. In the analysis it was checked that the individual events are kinematically complete. The efficiency to detect an event with four photons in the final state and to reconstruct it in the analysis chain is typical 50%, for eight photons it is about 20%.

In the four-photon final state we plot the momentum of any pair of two photons Fig. 2(a). The momentum distribution is dominated by $\bar{p}p \to \pi^0\pi^0$. The fit to the data in the momentum range is displayed inset. Also seen is a smaller peak due to the reaction $\bar{p}p \to \pi^0\eta$, seen better in Fig. 2(b) which excludes the $\pi^0\pi^0$ peak (the fit to the data is again shown inset).

The momenta for the two reactions $\bar{p}p \to \eta\eta$ and $\bar{p}p \to \pi^0\omega$ are rather close, and both reactions contribute to the 4γ final state. In the latter annihilations, a low-energy photon from $\omega \to \pi^0\gamma$ may be lost, the 4C fit then detunes the kinematics slightly and the π^0 momenta are shifted, obscuring the weak signal from $\bar{p}p \to \eta\eta$ events. In our data (Fig. 2(b)) we indeed see an asymmetric structure at about 760 MeV/c. The background from $\pi^0\omega$ is eliminated by requiring both $\gamma\gamma$ pairs to have a mass of more than 200 MeV/c^2 (Fig. 2(c)); an undistorted signal due to $\bar{p}p \to \eta\eta$ is now clearly visible.

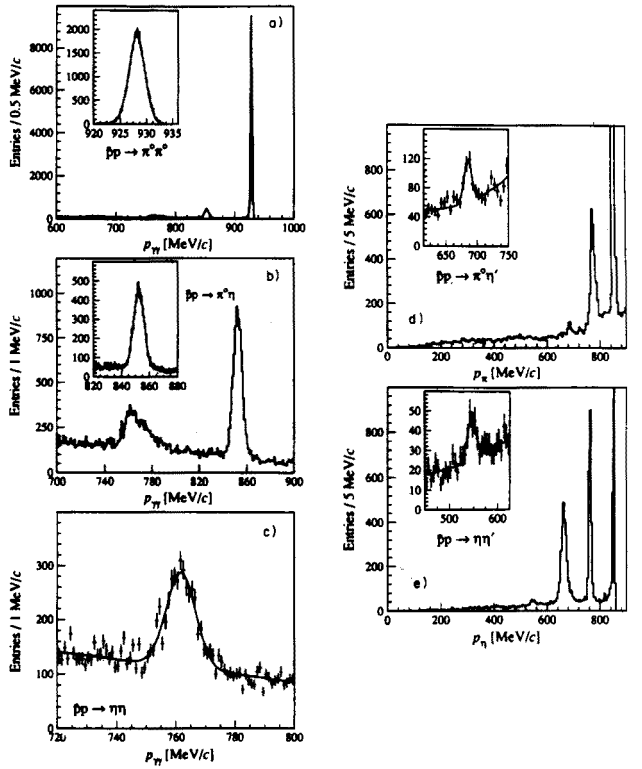

Fig. 2. $\bar{p}p \to 4\gamma$ (*zero-prong* trigger data). (a) $\gamma\gamma$ momentum distribution (6 entries per event). (b) Same with suppression of the signal for $\pi^o\pi^o$. (c) Same as (b) where the $\gamma\gamma$ pairs have an invariant mass greater than 200 MeV/c^2. (d) Momentum of π^o in $\bar{p}p \to \pi^0\gamma\gamma$. (e) Momentum of η in $\bar{p}p \to \eta\gamma\gamma$. Insets show fits to the signals.

For $\bar{p}p \to \pi^0\eta'$ and $\eta\eta'$, we again use the 4γ final state and select $\gamma\gamma$ pairs with an invariant mass compatible with a π^0. We plot in Fig. 2(d) the π^0 momentum distribution showing three peaks (note that the expected $\pi^0\pi^0$ signal is out of the momentum range shown): $\pi^0\eta$ (the signal for which is so strong it passes off the vertical scale of the histogram), then $\pi^0\omega$ follows (with a lost photon), finally there is a small peak from $\pi^0\eta'$. The inset shows an expanded view of the π^0 momentum distribution in the region where the signal from $\pi^0\eta$ is expected. By similarly plotting the η momentum spectrum we observe $\bar{p}p \to \eta\eta'$ jointly with $\pi^0\eta$, $\eta\eta$, and $\eta\omega$ (Fig. 2(e)).

An important aspect of the analysis is the fact that most of these reactions can also be observed in the final state containing eight photons. These events are kinematically fit to three hypotheses: (A) $\pi^0\pi^0\pi^0\pi^0$, (B) $\pi^0\pi^0\pi^0\eta$ and (C) $\pi^0\pi^0\eta\eta$. The π^0 momentum distribution of class (A)

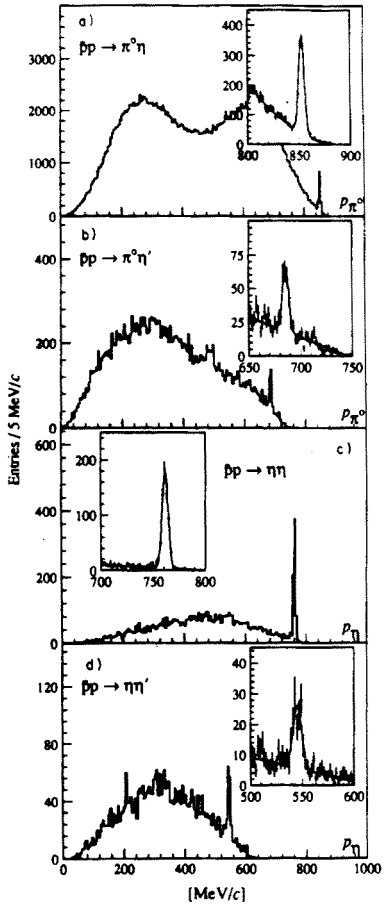

Fig. 3. (a) π^0 momentum in $\bar{p}p \to \pi^0\pi^0\pi^0\pi^0$. (b) and (c) are respectively the π^0 and η momenta in $\bar{p}p \to \pi^0\pi^0\pi^0\eta$. (d) η momentum in $\bar{p}p \to \pi^0\pi^0\eta\eta$. Fits are shown inset.

events is shown in Fig. 3(a) (4 entries per event), and of class (B) in Fig. 3(b) (3 entries per event). The two distributions show peaks originating from the reactions $\bar{p}p \to \pi^0\eta$ and $\pi^0\eta'$ respectively. The number of events is determined from a fit (see insets). The reactions $\bar{p}p \to \eta\eta$ and $\eta\eta'$ are observed by plotting the η momentum distribution of class (B) and class (C) events (Figs 3(c) and 3(d) respectively). The efficiency for detection of one of these reactions is determined from Monte Carlo simulations. Thus branching ratios for the reactions can be determined. The results from the two different final states agree, after efficiency corrections, very well demonstrating the good understanding of the detector which has been achieved. The final results are given in [16]. Here we give only those ratios of branching ratios

relevant for the present discussion.

$$\frac{BR(\bar{p}p \to \pi^0\eta')}{BR(\bar{p}p \to \pi^0\eta)} = 0.548 \pm 0.046 \pm 0.014 \pm 0.028\,,$$

$$\frac{BR(\bar{p}p \to \eta\eta')}{BR(\bar{p}p \to \eta\eta)} = 1.309 \pm 0.127 \pm 0.032 \pm 0.067\,,$$

$$\frac{BR(\bar{p}p \to \omega\eta')}{BR(\bar{p}p \to \omega\eta)} = 0.515 \pm 0.028 \pm 0.013 \pm 0.026\,.$$

The first error is statistical, the second systematic and the third is due to uncertainties in meson decay branching fractions that do not cancel in the ratios. The η and η' wave functions are defined as follows:

$$|\eta\rangle = X_\eta \frac{1}{\sqrt{2}}|u\bar{u} + d\bar{d}\rangle + Y_\eta|s\bar{s}\rangle\,,$$

$$|\eta'\rangle = X_{\eta'}\frac{1}{\sqrt{2}}|u\bar{u} + d\bar{d}\rangle + Y_{\eta'}|s\bar{s}\rangle \qquad \text{with}$$

$$\frac{X_{\eta'}}{X_\eta} = \cot^2\{\Theta_{PS} - \Theta_{ideal}\}\,.$$

The pseudoscalar mixing angle is then given by:

$$\frac{BR(\eta' X)}{BR(\eta X)} \cdot \frac{f_{dyn}(\eta X)}{f_{dyn}(\eta' X)} = \cot^2\{\Theta_{PS} - \Theta_{ideal}\}\,.$$

For $\Theta_{PS} = \Theta_{ideal} = 35.3°$ (the ideal mixing angle), η is a pure $s\bar{s}$ state and is supposed not to be produced (OZI rule). Note the inversion of the phase convention for pseudoscalar mesons.

From our data we can extract Θ_{PS} from three ratios. The three ratios should, of course, give consistent results on Θ_{PS}. We will see that this is the case only for some dynamical corrections, not for others. A complete list of tests can be found elsewhere; here I demonstrate the principle using a few examples.

The dynamical factor f_{dyn} should contain two components, the phase space factor q and the momentum dependence of the amplitude T for the annihilation process. For small momenta, $T \sim q^l$, and

$$f_{dyn} = q^{(2l+1)}\,.$$

Annihilation into $\eta\omega$ and $\eta'\omega$ can occur from the $^3S_1$ and $^1P_1$ states, but here we neglect a possible contribution of P-wave annihilation [17].The angular momentum between the two outgoing mesons is then $l = 1$ and the

dynamics are sensitive to centrifugal barrier factors. Annihilations into two pseudoscalar mesons are allowed from the $^3P_0$ and $^3P_2$ states of $\bar{p}p$ atoms requiring $l = 0$ and $l = 2$, respectively. We assume that the two states contribute to the process according to their statistical weights. The three determinations of Θ_{PS} give incompatible results, with a $\chi^2/N_F = 46.7$. We consider this as completely unacceptable.

Vandermeulen [4] suggested a very successful model in which he assumed that the annihilation process prefers small energy transfers to the outgoing mesons. In his model, for two mesons with masses m_a and m_b,

$$f_{\mathrm{dyn}} = q \cdot \exp\{A(s - (m_a + m_b)^2)^{1/2}\},$$

where $s = 4m_p^2$ and $A = -1.2\,\mathrm{GeV}^{-1}$ is obtained from a fit to data. With this assumption, he obtains a good description of $\bar{p}p$ annihilation in flight into multi-particle final states. We find that this model gives a consistent result for Θ_{PS} with a χ^2 of 1.6 and a resulting mixing angle of $-19.8°$.

Obviously low-energy $\bar{p}p$ annihilations do not favour high momenta. Therefore I used a very simple dynamical model [12] to extract the isospin decomposition of the $\bar{p}p$ atomic wave function;

$$f_{\mathrm{dyn}} = 1\,.$$

This assumption yields a consistent result for Θ_{PS}.

By varying the parameter A in (1) we find a best fit to the data with $A = -0.83\,\mathrm{GeV}^{-1}$, $\chi^2 = 1.1$ ($N_F = 1$) and

$$\Theta_{PS} = -(17.3 \pm 1.8)°\,.$$

This latter value is given as final result in [18].

5. Conclusions

The abundant production of η and η' mesons in $\bar{p}p$ annihilation at rest in different reactions permits to determine the pseudoscalar mixing angle with an accuracy comparable to that of other experiments. Since the value of the mixing angle ($\sim -10°$ as derived from the quadratic mass formula or $\sim -20°$ as suggested by the linear mass formula) has been controversial for a long time, this new determination is interesting in itself. Personally, I find it even more interesting that it is possible to overcome the difficulties of a complicated process in hadrophysics, of annihilation dynamics. It is generally believed that the NNη' coupling is much weaker than the NNη coupling. In a concrete situation where we deal with exclusive reactions we find that the relative production rates for η' and η mesons are completely

governed by their respective quark contents. Further, we get a consistent result on Θ_{PS} only assuming a rather peculiar dependence of production rates on the available phase space [4, 12]. In my interpretation this fact warns us that annihilation is not a a reaction in which elementary particles annihilate and new particles are created: annihilation is a few-body problem with its own dynamical consequences. Nobody would assume that the internal Auger effect should prefer ejection of electrons with high momenta; the inverse statement holds true. In my view, $\bar{p}p$ atoms annihilate by annihilation and recreation of quark–antiquark pairs, and by rearrangement of the constituent quarks and antiquarks. This process resembles much more Auger processes than decays of one heavy particle which needs to be described at the level of the underlying dynamics.

The onset of the validity of perturbative QCD is usually assumed to occur at about 2 GeV, since scaling sets in at about $4(\text{ GeV})^2$. However, the region below $4(\text{ GeV})^2$ is governed by resonance production, hence deviations from scaling are no proof against the assumption that perturbative QCD might be applicable at even lower momentum transfers. The surprising success of QCD related calculations of the light-meson mass spectrum [19] supports this conjecture. High-statistics study of particle production at COSY might therefore reveal that hadrodynamics is simpler than we assume at present, that particle production is governed by reactions which need to be described at the quark level.

REFERENCES

[1] E. Klempt, *Physica Scripta* **43**, 65 (1991).
[2] S. van der Meer, *Rev. Mod. Phys.* **57**, 689 (1985).
[3] C. Amsler *et al.*, *Phys. Lett.* **B297**, 214 (1992).
[4] J. Vandermeulen, *Z. Phys.* **C37**, 563 (1988).
[5] S. Mundigl, M.V. Vacas, M. Weise, *Z. Phys.* **A338**, 103 (1991).
[6] T. Hippchen, J. Haidenbauer, K. Holinde, V. Mull, *Phys. Rev.* **C44**, 1337 (1991).
[7] C.B. Dover, T. Gutsche, M. Maruyama, A. Faessler, *Prog. Part. Nucl. Phys.* **29**, 87 (1992).
[8] E. Klempt, *Phys. Lett.* **B**, (1993).
[9] C. Dover, P. Fishbane, *Nucl. Phys.* **B244**, 349 (1984).
[10] M. Kohno, W. Weise, *Phys. Lett.* **B152**, 303 (1985).
[11] M. Maruyama, S. Furui, A. Faessler, *Nucl. Phys.* **A472**, 643 (1987).
[12] E. Klempt, *Phys. Lett.* **B244**, 122 (1990).
[13] C. Dover, J.M. Richard, J. Carbonell, *Phys. Rev.* **C44**, 1281 (1991).
[14] T. Hippchen, K. Holinde, W. Plessas, *Phys. Rev.* **C39**, 761 (1989).
[15] E. Aker *et al.*, *Nucl. Instr. Meth.* **A321**, 69 (1992).
[16] C. Amsler *et al.*, *Z. Phys.* **C58**, 175 (1993).

[17] G. Reifenröther, E. Klempt, *Phys. Lett.* **B245**, 129 (1990).
[18] C. Amsler *et al.*, *Phys. Lett.* **B294**, 451 (1992).
[19] St. Godfrey, N. Isgur, *Phys. Rev.* **D32**, 189 (1985).